# Investigations on Solid Chlorine Dioxide: Temperature-Dependent Crystal Structure, IR Spectrum, and Magnetic Susceptibility

**Anette Rehr and Martin Jansen***

Institute of Inorganic Chemistry, University of Bonn, Gerhard-Domagk-Strasse 1, 5300 Bonn 1, Germany

*Received February 27, 1992*

Single crystals of chlorine dioxide were grown in situ on a four-circle diffractometer, and the crystal structures were solved at five different temperatures (–75, –90, –110, –130, and –150 °C). At –150 °C, the crystal system, space group, unit cell parameters, and $R$ factor are as follows: orthorhombic, *Pbca*, $a$ = 10.767 (12) Å, $b$ = 6.654 (3) Å, $c$ = 5.518 (1) Å, $V$ = 395.29 (48) Å$^3$, $Z$ = 8, $R$ = 0.024. In the solid state, the $ClO_2$ molecules associate to form weakly bonded dimers which are "head to tail" with respect to one Cl–O bond. The intermolecular interaction was confirmed by magnetic measurements, which show a steep decrease to negative $\chi$ values below –93 °C, and by IR spectroscopy.

## Introduction

Radical molecules and ions are relatively rare in the chemistry of main group elements but seem to occur more frequently for triatomic entities having 19 electrons. Among these are $O_3^-$,[1] $S_3^-$,[2] $P_3^{4-}$,[3] $NF_2$,[4] $SO_2^-$,[5] and $ClO_2$, which all have varying tendencies to dimerize.

Bent $AB_2$ molecules, which possess 19 valence electrons, show little tendency to dimerize through the formation of A–A bonds because of repulsive interactions between the nonbonding electron pairs located at the A atoms. This is supported by the fact that the tendency to dimerize increases when the repulsion of the nonbonding electrons is reduced, which might be effected, for example, by polarization. Thus, stable dimers form when the differences between the electronegativities of A and B ($\Delta_{AB}$) are greater than or equal to 1.0. Examples are $2NF_2 = N_2F_4$ or $2SO_2^- = S_2O_4^{2-}$.

Thus, $ClO_2$ ($\Delta_{AB}$ = 0.5) should not exist as a dimer, and it has been reported that there are no indications at all for a dimerization of $ClO_2$.[6] Another feature of these 19-electron systems rendering dimerization more difficult is that the unpaired electron is occupying the $2b_1$ ($\pi^*$) molecular orbital, which affords considerable electronic reorganization when forming a Cl–Cl $\sigma$-bond. To gain insights into this problem for solid $ClO_2$, we have performed X-ray crystal structure determinations, recorded the IR spectra, and determined the magnetic susceptibilities at different temperatures.

## Experimental Section

**Apparatus.** Chlorine dioxide was handled in a glass vacuum line lubricated with Kel-F grease. Infrared spectra were recorded in the range 4000–40 cm$^{-1}$ on a Bruker IFS 113 v spectrometer. Spectra of the solids (–196 to –60 °C) were obtained by condensing $ClO_2$ onto Si and KBr windows, and spectra of gases, by using a cell of 10-cm length with Si windows. The magnetic susceptibility was measured in a SQUID magnetometer (Type 130, Fa. Quantum Design, San Diego). For this purpose, the substance was condensed into a quartz capillary to a height of 3–4 mm.

**X-ray Diffraction.** The single crystals were grown in capillaries (o.d. = 0.3 mm) in situ on a CAD-4 four-circle diffractometer. The capillaries were filled by distilling $ClO_2$ from a cold trap (–50 °C) into a capillary tube (–120 °C) which previously was cleaned with aqua regia. Then both source and filled capillary tube were cooled to –196 °C, and the capillary was sealed under vacuum. Storage and transfer to the diffractometer were carried out with continuous cooling at –196 °C.

Prior to crystal growth via a modified Stockbarger–Bridgeman[7] technique, the contents of the capillary tube were purified by several fast cycles of zone melting from bottom to top. Temperature control was achieved by balanced heating (radiation of an IR lamp focused at the sample by a concave mirror) and cooling (laminar flow of cold $N_2$, standard Nonius cooling device). For crystal growth, the focussed IR spot was moved slowly (1 mm h$^{-1}$), from bottom to top along the part in the middle of the purified region (0.5-mm portions at both ends were left out). The quality of the single-crystal zone formed was checked by X-ray diffraction (oscillation photographs). Data collections were carried out at –75, –90, –110, –130, and –150 °C, respectively. In each case, the lattice constants were refined using 25 reflections, each measured at positive and negative diffraction angle $\theta$. The experiments were difficult to perform; thus not all crystals at all temperatures gave sets of data of equal quality. In particular the –110 °C refinement yielded slightly higher esd's for the bond lengths. No absorption correction was performed ($\mu$(Mo K$\alpha$ = 14 cm$^{-1}$)), because (i) the shape of the crystal that had formed in the capillary tube was irregular and (ii) the semiempirical method via $\psi$ scans failed as a consequence of restrictions on $\chi$ imposed by the cooling nozzle. The intensities were corrected for Lorentz and polarization effects. By Laue symmetry (*mmm*) and systematic extinctions, the space group is unequivocally fixed as *Pbca*. The structure was solved by direct methods, and all data sets were refined by using full-matrix least-squares procedures and applying anisotropic temperature factors to all atoms. All calculations were performed on a Micro VAX computer using the SHELX/SHELXS[8] program systems. Further experimental details appear with the crystal data in Table I or in the supplementary material, while positional parameters (–150 °C) are given in Table II.

**Materials.** Commercial chlorine, $NaClO_2 \cdot 3H_2O$ (Janssen), and $P_2O_5$ (Baker) were used as received.

*Warning*! Chlorine dioxide is extremely explosive. At temperatures below –40 °C and pressures below 50 mbar, it is relatively safe to handle. When $ClO_2$ was handled, exposure to light was avoided if possible. Otherwise, all operations were carried out under red light. The apparatus should be painstakingly cleaned prior to use.

(1) Schnick, W.; Jansen, M. *Angew. Chem.* **1985**, *97*, 48; *Angew. Chem., Int. Ed. Engl.* **1985**, *24*, 54. Schnick, W.; Jansen, M. *Rev. Chim. Miner.* **1987**, *24*, 446. Hesse, W.; Jansen, M.; Schnick, W. *Prog. Solid State Chem.* **1989**, *19*, 47.
(2) Seel, F.; Güttler, H. J.; Simon, G.; Wieckowski, A. *Pure Appl. Chem.* **1977**, *49*, 45. Fuginaga, T.; Kowamoto, T.; Okazaki, S.; Hojo, M. *Bull. Chem. Soc. Jpn.* **1980**, *53*, 2851.
(3) von Schnering, H. G.; Hartweg M.; Hartweg, V.; Hönle, W. *Angew. Chem.* **1989**, *101*, 98; *Angew. Chem., Int. Ed. Engl.* **1989**, *28*, 56.
(4) Freemann, J. P. *Inorg. Chim. Acta, Rev.* **1967**, *1*, 65.
(5) Clark, H. C.; Horsfield, A.; Symons, M. C. R. *J. Chem. Soc.* **1961**, 7.
(6) Pascal, J.-L.; Pavia, A. C.; Portier, J. *J. Mol. Struct.* **1972**, *13*, 38.
(7) Bridgeman, P. W. *Proc. Am. Arts Sci.* **1925**, *60*, 305. Stockbarger, D. C. *J. Opt. Soc. Am.* **1937**, *27*, 416.
(8) Sheldrick, G. M. SHELX-76, Program for crystal structure determination. University of Cambridge, England, 1976. SHELXS-86, Program for solving crystal structures. University of Göttingen, Germany, 1986.
(9) Brauer, G. *Handbuch der Präparativen* Anorganischen Chemie, 3rd ed.; Enke: Stuttgart, Germany, 1974; p 312.

0020-1669/92/1331-4740$03.00/0 

**Table I.** Crystallographic Data for $ClO_2$

| space group | *Pbca* | *Pbca* | *Pbca* | *Pbca* | *Pbca* |
|---|---|---|---|---|---|
| $a$ (Å) | 10.767 (12) | 10.784 (13) | 10.818 (5) | 10.820 (10) | 10.869 (10) |
| $b$ (Å) | 6.654 (3) | 6.675 (3) | 6.673 (3) | 6.701 (2) | 6.714 (4) |
| $c$ (Å) | 5.518 (1) | 5.538 (1) | 5.552 (1) | 5.567 (1) | 5.585 (3) |
| $V$ (Å$^3$) | 395.29 (48) | 398.59 (5) | 400.80 (29) | 403.60 (41) | 407.54 (52) |
| $Z$ | 8 | 8 | 8 | 8 | 8 |
| $T$ (°C) | −150 | −130 | −110 | −90 | −75 |
| λ (Å) | | | 0.710 69 | 0.710 69 | 0.710 69 |
| $d_{calc}$ (g/cm$^3$) | | | | | 2.24 |
| $\mu$ (cm$^{-1}$) | | | | | 13.65 |
| $R^a$ (%) | 2.4 | 3.1 | 5.2 | 4.4 | 3.2 |
| $R_w{}^b$ (%) | 2.3 | 3.0 | 4.6 | 4.3 | 3.0 |

$^a$ $R = \sum||F_o| - |F_c||/\sum|F_o|$. $^b$ $R_w = [\sum w(|F_o| - |F_c|)^2/\sum w(F_o)^2]^{1/2}$.

**Table II.** Positional Coordinates (at −150 °C) and Equivalent Isotropic Displacement Coefficients (Å$^2$ × 10$^4$)

| atom | $x/a$ | $y/b$ | $z/c$ | $U_{eq}{}^a$ |
|---|---|---|---|---|
| Cl1 | 0.615 16 (4) | 0.484 78 (6) | 0.193 22 (8) | 176 (2) |
| O1 | 0.712 01 (12) | 0.347 80 (20) | 0.103 31 (26) | 254 (7) |
| O2 | 0.491 13 (12) | 0.394 51 (19) | 0.227 05 (25) | 218 (6) |

$^a$ $U$ given as one-third of the trace of the $U_{ij}$ tensor.

**Preparation of $ClO_2$.** The synthesis was carried out according to Brauer.[9] The resulting $ClO_2$ was dried by passing it over $P_2O_5$ and collected at −196 °C. Subsequently, it was purified by fractional condensation through traps at −90, −120, and −196 °C. The contents of the −120 °C trap were used for further investigations.

## Results and Discussion

At a first glance, the crystal structure of $ClO_2$ consists of isolated molecules. The Cl–O bond lengths and the O–Cl–O angle are similar to the values found for gaseous $ClO_2$ (1.469 84 (1) Å, 117.403 (3)°);[10] however, the differences for the bonding angles are significant. This and the observation that the bonds between chlorine and the crystallographically independent oxygen atoms are different are indications of the presence of solid-state effects. A closer inspection of the molecular packing reveals that it is not governed exclusively by packing effects.

Thus, in contrast to the structure of solid $SO_2$,[11] where the baricenters of the molecules are arranged according to the motif of a cubic closest packing, the crystal structure of $ClO_2$ does not show any relation to one of the close packings. In addition, in $SO_2$, the electric dipoles are ordered in a ferroelectric sense, while they are antiferroelectrically ordered in $ClO_2$. Finally, the most pronounced difference documents itself in the shortest intermolecular contacts. In solid $SO_2$, they are fairly uniform within the range expected for van der Waals interactions, whereas in $ClO_2$, one of them (Cl–O2′) is shortened significantly to 2.71 Å when compared to the remaining ones, which range from 3.00 to 3.30 Å. As the relative reduction of the intermolecular Cl–O2 bond length is virtually the same as that found in solid NO for side-on dimerization (∼10%),[12] we attribute this effect to a "head to tail" dimerization (with respect to the Cl–O2 bond) of two entities of $ClO_2$. The dimer formation across a center of symmetry in *Pbca* is depicted in Figure 1. The dihedral angle O1–Cl–O2–Cl′ is 101.9°. The formation of dimers in $ClO_2$ may not be explained by interaction of the electric dipoles because intermolecular association is not observed in solid $SO_2$, which shows a greater electric dipole moment. Thus the most likely explanation is to assume electronic interactions mediated by the HOMO ($2b_1$) accommodating the unpaired electron. Indeed, the mutual orientation of the $ClO_2$ molecules allows for an overlap of the p-orbitals perpendicular to the planes through Cl, O1, and O2 of the monomers. Additional support for this view is given by the angle O2–Cl···O2′ being 81°.

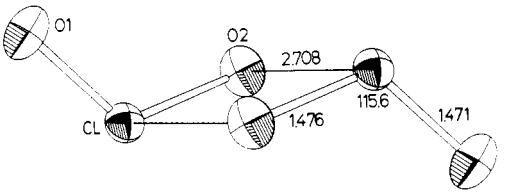


**Figure 1.** The $ClO_2$ dimer with a center of symmetry.

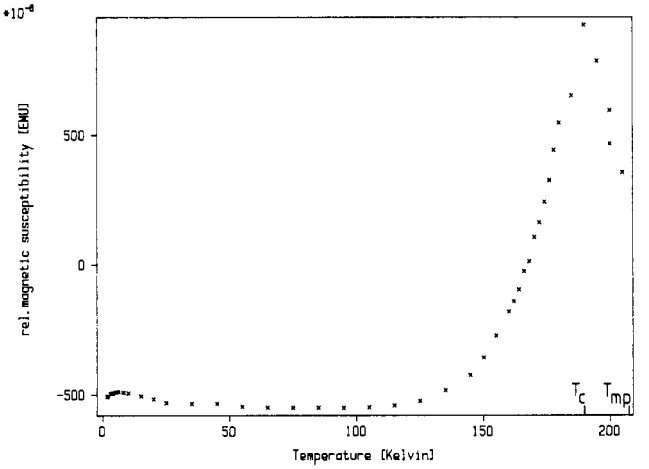


**Figure 2.** Magnetic susceptibility of $ClO_2$.

**Table III.** Interatomic Distances (Å) and Bond Angles (deg)

| | −75 °C | −90 °C | −110 °C | −130 °C | −150 °C |
|---|---|---|---|---|---|
| Cl–O1$^a$ | 1.464 (2) | 1.465 (2) | 1.464 (3) | 1.469 (1) | 1.471 (1) |
| Cl–O2$^a$ | 1.469 (2) | 1.469 (2) | 1.475 (3) | 1.476 (1) | 1.476 (1) |
| Cl–O2$^b$ | 2.778 (2) | 2.758 (3) | 2.740 (3) | 2.721 (2) | 2.708 (2) |
| Cl–O2 | 3.028 (2) | 3.019 (3) | 3.004 (3) | 3.001 (2) | 2.989 (2) |
| Cl–O1 | 3.134 (2) | 3.121 (3) | 3.108 (3) | 3.103 (2) | 3.089 (2) |
| Cl–Cl$^b$ | 3.353 (2) | 3.328 (2) | 3.312 (2) | 3.292 (2) | 3.277 (2) |
| O1–O2$^a$ | 2.490 (3) | 2.488 (3) | 2.491 (4) | 2.492 (3) | 2.494 (3) |
| O1–O1 | 3.101 (3) | 3.088 (3) | 3.075 (4) | 3.071 (3) | 3.051 (3) |
| O1–O2 | 3.193 (3) | 3.179 (3) | 3.177 (4) | 3.178 (4) | 3.163 (4) |
| O2–O2$^b$ | 2.917 (3) | 2.907 (3) | 2.898 (4) | 2.885 (3) | 2.879 (3) |
| O1–Cl–O2 | 116.2 (1) | 116.0 (1) | 116.0 (2) | 115.6 (1) | 115.6 (1) |

$^a$ Intramolecular. $^b$ Intradimer.

This dimerization should result in a spin compensation, and the crystalline $ClO_2$ should become diamagnetic. This expectation was verified, indeed, by determining the magnetic susceptibility as shown in Figure 2. Below a surprisingly high temperature ($T_c$) of −84 °C, $ClO_2$ becomes diamagnetic whereas, above $T_c$ up to its melting point, solid $ClO_2$ behaves paramagnetically. In order to check whether a structural phase transition occurs on passing $T_c$, we have determined the crystal structure at five different temperatures, some below and some above $T_c$. The observed bond lengths and bond angles are given in Table III. In general, shorter bonds are affected less than longer ones by thermal shrinkage or expansion of molecular solids. The behavior of the intramolecular Cl–O bonds thus is as expected. However, the next shortest bond Cl–O2′ (forming the dimer) shows a stronger shortening on passing to the magnetically ordered state than all the remaining (longer) intermolecular contacts. There are two further structural features giving support for the proposed intermolecular interactions between adjacent molecules. If there is significant overlap of the p-orbitals contributing to the antibonding MO ($2b_1$), this should lead to an increase of antibonding electron density along the Cl–O2 bond and thus weaken it, which is actually observed. Admittedly, this latter effect is close to the limits of experimental error.

(10) Miyazaki, K.; Tanoura, M.; Tanaka, K.; Tanaka, T. *J. Mol. Spectrosc.* **1986**, *116*, 435.
(11) Post, B.; Schwartz, R. S.; Fankuchen, I. *Acta Crystallogr.* **1952**, *5*, 372.
(12) Dulmage, W. J.; Meyers, E. A.; Lipscomb, W. N. *Acta Crystallogr.* **1953**, *6*, 760. Lipscomb, W. N.; Wang, F. E.; May, W. R.; Lippert, E. L. *Acta Crystallogr.* **1961**, *14*, 1100.

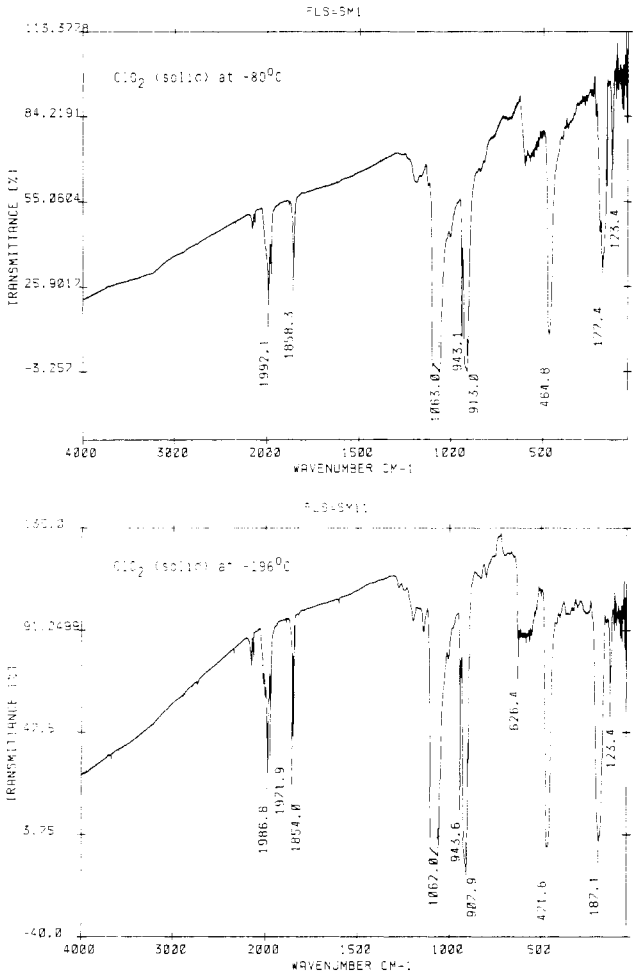


**Figure 3.** Infrared spectra of solid $ClO_2$ at −196 and −80 °C.

**Table IV.** IR Data for $ClO_2$

| gas, room temp | crystalline, −196 °C | crystalline, −80 °C |
|---|---|---|
| 1108 $\nu_{as}(B_2)$ | 1062 $\nu_{as}(B_2)$ | 1063 |
| 943 $\nu_s(A_1)$ | 908 $\nu_s(A_1)$ | 913 |
| 447 $\delta(A_1)$ | 471 $\delta(A_1)$ | 465 |
| | 187 (intradimer) | 177 |
| | 123 (lattice mode) | 123 |

The infrared spectra of solid $ClO_2$ at −196 and −80 °C (Figure 3, Table IV; the data for gaseous $ClO_2$ are included for comparison) quite clearly show the three internal modes in the expected frequency range from 1300 to 450 $cm^{-1}$. Below 450 $cm^{-1}$, there is one band at a surprisingly high frequency (187 and 177 $cm^{-1}$, respectively) which we attribute to the antisymmetric stretch vibration of the $Cl_2O_2$ ring in the dimer. As expected, the frequency of this mode increases with decreasing distance of the $ClO_2$ bridge and decreasing temperature. The experimental findings give clear evidence for intermolecular interactions between adjacent $ClO_2$ molecules yielding dimers of point symmetry $C_i$. All observations, including the seemingly contradictory features that structural properties and vibrational behavior give indications for dimerization from below the melting point at −59 °C, whereas spin compensation does not occur until cooling below −84 °C, may be explained by assuming some degree of overlap of parts of the $\pi$-orbitals constituting the antibonding MO's ($2b_1$) of the monomers. With respect to the dimer ($C_i$), two MO's of symmetries $a_u$ (bonding) and $a_g$ (antibonding) result. The two lowest lying states generated by population of $a_u$ and $a_g$ by two electrons are $^1A_g$ and $^3A_u$. As the overlap of the orbitals involved is only small, the separation of $^1A_g$ and $^3A_u$ should also be small and both might be populated at the melting point. With decreasing temperature, the population of $^3A_u$ also decreases, and eventually, only the diamagnetic state $^1A_g$ is occupied, resulting in diamagnetism.

## Conclusions

The crystal structure of $ClO_2$, determined at five different temperatures, gives evidence for the formation of head to tail dimers involving one of the two Cl–O bonds. This is supported by the observations of a band at relatively high frequency which is attributed to the stretching mode of the bridge.

Furthermore, spin compensation occurs at a surprisingly high temperature. The mutual orientation of the $ClO_2$ molecules allows for an overlap of p-orbitals perpendicular to the planes through the three atoms of the monomers. The MO's ($a_u$, $a_g$) and the temperature-dependent population of the resulting $^3A_u$ and $^1A_g$ states with two electrons are used to explain the observed changes in the magnetic and spectroscopic properties.

**Acknowledgment.** This work was supported by the Fonds der Chemischen Industrie and by the DFG (Leibniz Programm). Assistance from Dr. J. Arlt, Dipl. Chem. St. Hagen, and Dipl. Ing. N. Wagner with the recording of the IR spectra and the determination of the magnetic properties is gratefully acknowledged.

**Supplementary Material Available:** Tables giving unit cell parameters, atom coordinates, anisotropic thermal parameters, bond lengths, and bond angles (4 pages). Ordering information is given on any current masthead page.

**Registry No.** Chlorine dioxide, 10049-04-4.